CALCULATION OF THE APPARENT MASS OF A SUPERSONIC GAS JET

A. L. Isakov and A. S. Stepanov

UDC 533.607.11

The authors compute the amount of air ejected from supersonic nonisothermal underexpanded jets. The results are compared with test data.

Prandtl theory is used in [1, 2] to examine a method of calculating the apparent mass of a jet discharging under design conditions. The mixing constants for the entrance and main sections of the jet ($b_1 = 0.27$ and $b_1 = 0.22$, respectively) were determined from tests with incompressible jets. However, as was shown by comparing the results of calculation with experiments, even for cold air jets the value of the mixing constant b_1 depends on the Mach number at the nozzle exit M_a, and there are no data to take account of the influence of the degree of preheating on the ejection capability of nonisothermal underexpanded jets.

From an experimental investigation of the ejection capacity of supersonic gas jets [3] one can determine the apparent mass of these jets discharging into an immersed medium (air) from contoured nozzles ($\alpha_a = 0$) with exit Mach number $M_a = 1.53$-3.03 and degree of underheat of the gas $\bar{\theta}^* = 1$-6.9. A section of the jet of length $\bar{x} = 1$-9 was investigated, the combustion products with the above degree of underheat had $k_a = 1.4$-1.277, respectively, and the degree of underexpansion was varied in the range $n = 0.6$-2.06.

From these experiments we determined the coefficient b_1 for the design discharge condition ($n = 1$). The dependence of the mixing constant on the degree of underheat is increasing in character: for an increase of jet stagnation temperature from $T_0 = 300°K$ to $T_0 = 1900°K$ the coefficient b_1 decreases by roughly a factor of 2 to 3 (Fig. 1). In addition, the coefficient b_1 has different values for the different mixing zones. One of the dependences $b_1(\bar{x})$ represented in Fig. 2 for $M_a = 1.53$ illustrates this. It can be seen that in the entrance section of the design jet (to the left of the broken line, $\bar{x} \le \bar{x}_{ent}$) this relation is complex, and outside the entrance section, i.e., in the transition and main sections (to the right of the broken line, $\bar{x} > \bar{x}_{ent}$) the coefficient b_1 remains practically constant for $\bar{\theta}^* = \text{const}$.

By reducing the experimental data one can obtain the coefficient b_1 as a function of the parameters $\bar{\theta}^*$, $\bar{x}$, $a\lambda_a^2$ for the entrance section ($\bar{x} \le \bar{x}_{ent}$):

$$b_1 = \exp A' + B' \ln \bar{x} + C'\bar{x}, \tag{1}$$

where

$$A' = -1.597\, a\lambda_a^2 - 0.106\,\bar{\theta}^* + 1.09\,(a\lambda_a^2)^2 + 0.352\cdot 10^{-2}\,(\bar{\theta}^*)^2 + 0.904\cdot 10^{-1}\, a\lambda_a^2\,\bar{\theta}^* + 0.77\cdot 10^{-2}\,(a\lambda_a^2\,\bar{\theta}^*)^2 + 0.788;$$

$$B' = 1.381\, a\lambda_a^2 + 0.858\cdot 10^{-1}\bar{\theta}^* - 1.207\,(a\lambda_a^2)^2 + 0.152\cdot 10^{-2}\,(\bar{\theta}^*)^2 - 0.28\, a\lambda_a^2\,\bar{\theta}^* + 0.237\cdot 10^{-1}\,(a\lambda_a^2\,\bar{\theta}^*)^2 - 0.34;$$

$$C' = -0.177\cdot 10^{-1}\, a\lambda_a^2 - 0.539\cdot 10^{-2}\bar{\theta}^* + 0.44\cdot 10^{-1}\,(a\lambda_a^2)^2 + 0.138\cdot 10^{-2}\,(\bar{\theta}^*)^2 + 0.536\cdot 10^{-1}\, a\lambda_a^2\,\bar{\theta}^* - 0.688\cdot 10^{-2}(a\lambda_a^2\bar{\theta}^*)^2 - 0.414\cdot 10^{-2},$$

and for the main section ($\bar{x} > \bar{x}_{ent}$):

$$b_1 = 0.8406\cdot 10^{-1}\, a\lambda_a^2 - 0.2975\cdot 10^{-1}\,\bar{\theta}^* + 0.3571. \tag{2}$$

Leningrad Institute of Mechanics. Translated from Inzhenerno-Fizicheskii Zhurnal, Vol. 45, No. 3, pp. 365-370, September, 1983. Original article submitted March 1, 1982.

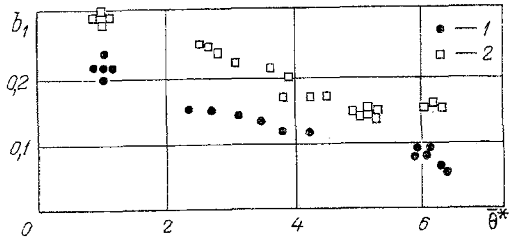

Fig. 1. Coefficient b_1 as a function of the relative temperature $\bar{\theta}^*$ (M_a = 2.03; n = 1; k_a = 1.40-1.28): 1) $\bar{x}$ = 1 (entrance section); 2) $\bar{x}$ = 6 (main section).

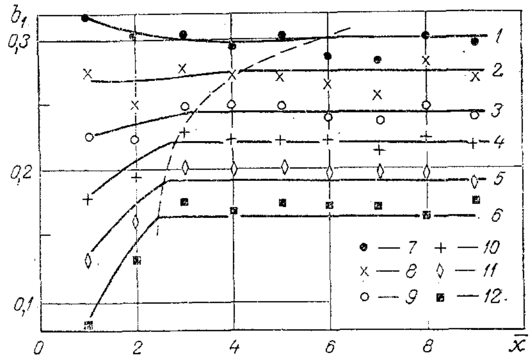

Fig. 2. Coefficient b_1 as a function of the axial distance $\bar{x}$ (M_a = 1.53; the solid curves show theory; the points show experiment; the broken line shows the length of the entrance section $\bar{x}_{ent}$): 1, 7) $\bar{\theta}^*$ = 1, k_a = 1.4; 2, 8) 2 and 1.344, respectively; 3, 9) 3 and 1.317; 4, 10) 4 and 1.30; 5, 11) 5 and 1.285; 6, 12) 6 and 1.277.

The values of b_1 determined from Eqs. (1) and (2) are shown by the solid line in Fig. 2. An estimate of the error of the approximations of Eqs. (1) and (2) (using the Fischer criterion) showed that it exceeds the error of measurement, but is not more than 13%.

The apparent mass of the design jet (n = 1) can be determined as the difference of the mass flow rates in the transverse section of the jet between the total flow rate Q_Σ and the flow rate of gas discharging through the nozzle Q_a [2, 4]. We can write the relative apparent mass as

$$q = \frac{Q_\Sigma - Q_a}{Q_a} = \frac{Q_{ab.at}}{Q_a} - 1 \tag{3}$$

or, after transformations,

$$q = k_1 \frac{x}{r_a} + k_2 \left(\frac{x}{r_a}\right)^2, \tag{4}$$

where

$$k_1 = b_1 [1 + \sigma\bar{\theta}^* (1 - a\lambda_a^2)] (A_1 - A_2);$$

$$k_2 = \left[b_1 \frac{1 + \sigma\bar{\theta}^* (1 - a\lambda_a^2)}{2} \right]^2 [A_2^2 + 2(A_0 - A_1 + A_0 A_1 - A_1 A_2) - A_0^2 - 2(A_{11} - A_{22})];$$

$$A_0 = \int_0^1 \frac{\rho}{\rho_0} d\eta; \quad A_1 = \int_0^1 \frac{\rho}{\rho_0} (1 - \eta^{3/2})^2 d\eta; \quad A_2 = \int_0^1 \frac{\rho}{\rho_0} (1 - \eta^{3/2})^4 d\eta;$$

$$A_{11} = \int_0^1 \frac{\rho}{\rho_0} \eta d\eta; \quad A_{22} = \int_0^1 \frac{\rho}{\rho_0} (1 - \eta^{3/2})^2 \eta d\eta.$$

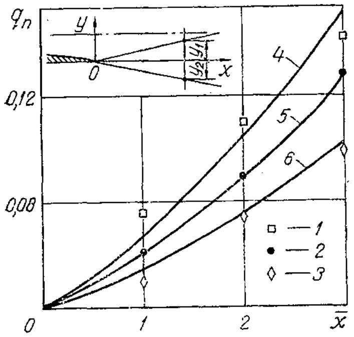

Fig. 3

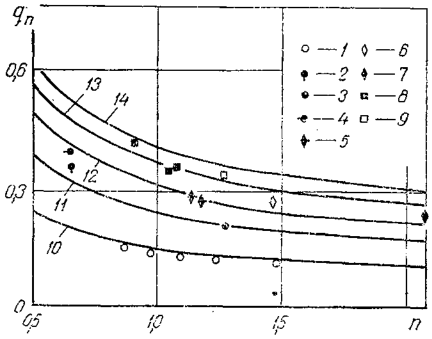

Fig. 4

Fig. 3. Variation of the apparent mass q_n of an isothermal jet as a function of the axial distance $\bar{x}$ ($n = 1.6$; $\bar{\theta}^* = 1$; $k_a = 1.4$; the solid lines are calculations using our technique; the points are experiments of [4]); 1, 4) $M_a = 1.53$; 2, 5) 2.03; 3, 6) 3.01.

Fig. 4. Variation of the apparent mass of a nonisothermal jet as a function of the degree of underexpansion n ($M_a = 2.03$; $\bar{x} = 1.75$; the solid lines are theory, the points are our experiment): 1, 10) $\bar{\theta}^* = 1$, $k_a = 1.4$; 2) 2.12 and 1.39, respectively; 3) 2.35 and 1.385; 4) 2.6 and 1.37; 5) 3.2 and 1.35; 6) 3.41 and 1.355; 7) 3.83 and 1.335; 8) 4.34 and 1.32; 9) 4.7 and 1.31; 11) 2.0 and 1.344; 12) 3.0 and 1.317; 13) 4.0 and 1.3; 14) 5.0 and 1.285.

For the boundary layer of a supersonic jet the dimensionless density, velocity, and temperature can be written in the following form [1]:

$$\frac{\rho}{\rho_0} = \frac{\bar{\theta}^*}{1 + (\bar{\theta}^* - 1)\eta} \cdot \frac{1 - a\lambda_a^2}{1 - \bar{\theta}^* a\lambda_a^2 \dfrac{[1 - (1 - \eta^{3/2})^2]^2}{1 + (\bar{\theta}^* - 1)\eta}},$$

$$\frac{u}{u_0} = 1 - (1 - \eta^{3/2})^2, \quad \frac{T}{T_0} = \frac{1}{\bar{\theta}^*} + \eta\left(1 - \frac{1}{\bar{\theta}^*}\right).$$

In the case of discharge of an underexpanded supersonic jet, if n differs only slightly from 1, one can postulate that the flow is quasiisobaric in the vicinity of the jet boundary. An analogous hypothesis was made in [5], and it was noted in [6] that a change of the densities of the jet and the medium by a factor of several did not change the universal nature of the profiles of velocity and temperature. On this basis we consider that under the above conditions, for the same stagnation temperatures, the rates of increase of the apparent mass along the design jet $(dq/dx)_{n=1}$ and the underexpanded jet $(dq_n/dx)_{n\neq 1}$ are the same, if the Mach number M_b is the same at the boundaries of these jets, i.e., if the condition can be written in the form

$$\left(\frac{dq}{dx}\right)_{n=1} = \left(\frac{dq_n}{dx}\right)_{n\neq 1} \tag{5}$$

for

$$(\bar{\theta}^*)_{n=1} = (\bar{\theta}^*)_{n\neq 1}, \tag{6}$$

$$(M_b)_{n=1} = (M_b)_{n\neq 1}. \tag{7}$$

Allowing for the fact that $(M_b)_{n=1} = (M_a)_{n=1}$, condition (7) can be rewritten as:

$$(M_a)_{n=1} = (M_b)_{n\neq 1}. \tag{8}$$

Then the apparent mass of an underexpanded jet is found from Eq. (5), allowing for Eq. (4):

$$q_n = \int_0^{S'} \left(\frac{dq}{dx}\right)_{n=1} dx = \int_0^{S'} \left(k_1 + 2k_2 \frac{x}{r_a}\right) dx = k_1 \frac{S'}{r_a} + k_2 \left(\frac{S'}{r_a}\right)^2, \ldots \tag{9}$$

where S' is the distance along the curved boundary of the underexpanded jet to the desired section. This means that the apparent mass of an underexpanded jet can be determined as the apparent mass of a design jet for which $M_a = M_b$ at the nozzle exit, i.e., instead of $\lambda_a(M_a)$ we substitute the value $\lambda_b(M_b)$, where for $n < 1$

$$M_b = \left\{ \frac{2}{k_a - 1} \left[\left(1 + \frac{k_a - 1}{2} M_a^2\right) n \frac{n + \frac{k_a + 1}{k_a - 1}}{1 + \frac{k_a + 1}{k_a - 1} n} - 1 \right] \right\}^{1/2},$$

and for $n > 1$

$$M_b = \left\{ \frac{2}{k_a - 1} \left[n^{\frac{k_a - 1}{k_a}} \left(1 + \frac{k_a - 1}{2} M_a^2\right) - 1 \right] \right\}^{1/2}.$$

The results of the calculations are shown in Figs. 3 and 4. When approximations (1) and (2) are used to determine the apparent mass of slightly underexpanded jets, the proposed relation (9) shows good agreement with different experimental data. Figure 3 shows the calculated curves, in comparison with the test data of [4], which investigated isothermal jets ($\overline{\theta}^* = 1$), i.e., jets of underheated air discharging into air at supersonic speeds.

An analogous comparison, but for nonisothermal jets, has also been made with our experiments conducted for this purpose at slightly underexpanded conditions (Fig. 4). These have also confirmed the validity of the suggested hypotheses and confirmed that one can use the relations proposed to calculate the apparent mass of supersonic jets with different degrees of underheat.

NOTATION

x, y, longitudinal and transverse coordinates; T_0, jet stagnation temperature; p_s, T_s, pressure and temperature of the surrounding air; $\overline{\theta}^* = T_0/T_s$, relative underheat temperature of the jet; d_a, r_a, diameter and radius of the nozzle exit; $\overline{x} = x/d_a$, relative jet length; k_a, adiabatic exponent; M_a, M_b, Mach number at the nozzle exit and at the jet boundary; p_a, pressure at the nozzle exit; $n = p_a/p_s$, degree of underexpansion of the jet discharge; b_1, mixing constant; x_{ent}, length of the jet entrance section; $\overline{x}_{ent} = x_s/d_a$, relative length of the entrance section; $\alpha = (k_a - 1)/(k_a + 1)$; λ, velocity coefficient; Q_Σ, total gas flow rate in a transverse section of the jet; Q_a, gas flow rate through the nozzle; $Q_{ab.m}$, absolute apparent mass of the jet; q, q_{un}, relative apparent mass of the design and underexpanded jets; ρ, u, T, density, velocity, and temperature of the gas in the jet boundary layer; ρ_0, u_0, density and velocity of the gas in the jet; y_1, y_2, transverse coordinates of the inner and outer edges of the boundary layer (Fig. 3); b, width of the boundary layer; η, dimensionless transverse boundary layer coordinate; σ, ratio of the molecular weights of the gases of the surrounding medium and the jet.

LITERATURE CITED

1. G. N. Abramovich, Theory of Turbulent Jets [in Russian], Fizmatgiz, Moscow (1960).
2. B. A. Balanin and V. M. Shlyakhtina, "Calculation of the mass in the entrance section of an underexpanded supersonic jet," in: Science Reports of LGU No. 396 [in Russian], Leningrad State Univ. (1973), p. 101.
3. A. L. Isakov and A. S. Stepanov, Investigation of the Electron Capacity of Supersonic Jets of Gas Discharging with a Slight Underexpansion [in Russian], Leningrad (1980); submitted by LMI to TsNII "Rumb," No. DR-1117; Sudostroenie, Ser. 1, No. 3, No. 189430 (1980).
4. B. A. Balanin, "The apparent mass of a supersonic jet under underexpanded discharge conditions," Inzh.-Fiz. Zh., 8, No. 5, 574 (1965).
5. G. N. Abramovich, "Investigation of an axisymmetric supersonic turbulent jet discharging from a nozzle with underexpansion," in: Investigation of Turbulent Jets of Air, Plasma and Real Gas [in Russian], Mashinostroenie, Moscow (1967).
6. G. N. Abramovich, Applied Gas Dynamics [in Russian], Nauka, Moscow (1976).